INTERNATIONAL JOURNAL OF PRECISION ENGINEERING AND MANUFACTURING Vol. 18, No. 4, pp. 587-597 APRIL 2017 / 587

REGULAR PAPER

DOI: 10.1007/s12541-017-0070-z
ISSN 2234-7593 (Print) / 2005-4602 (Online)

Development of a Rotary Clap Mechanism for Positive-Displacement Rotary Pumps: Experimental Verification and Optimization

Sung-Bo Shim[1,#], Young-Jun Park[2,3], Ju-Seok Nam[4], Su-Chul Kim[5], Jong-Mun Kim[6], and Kyeong-Uk Kim[2]

1 Upland-field Machinery Research Center, Kyungpook National University, 80, Daehak-ro, Buk-gu, Daegu, 41566, South Korea
2 Department of Biosystems and Biometerials Science and Engineering, Seoul National University, 1 Gwanak-ro, Gwanak-gu, Seoul, 08826, South Korea
3 Research Institute for Agriculture and Life Sciences, Seoul National University, 1 Gwanak-ro, Gwanak-gu, Seoul, 08826, South Korea
4 Department of Biosystems Engineering, Kangwon National University, 1 Kangwondaehak-gil, Chuncheon-si, Gangwon-do 24341, South Korea
5 Department of System Reliability, Korea Institute of Machinery and Materials, 1156, Gajeongbuk-ro, Yuseong-gu, Daejeon, 34103, South Korea
6 ClapMC Co., Ltd., 156, Gajeongbuk-ro, Yuseong-gu, Daejeon, 34103, South Korea
Corresponding Author / E-mail: environ80@naver.com, TEL: +82-53-950-7289, FAX: +82-53-950-7847

KEYWORDS: Pump performance, Rotary clap mechanism, Rotary pump comparison

We have developed a new positive-displacement type rotary clap pump. Its structure, working principles and pumping performances have been introduced and analyzed in the previous studies. In this study, the experiment using prototype rotary clap pump was conducted to verify the analyzed pump performances. The simulated flow rate, differential pressure, driving torque, and efficiencies for the prototype rotary clap pump were compared with the measurement results. We confirmed the applicability of the analysis model, because the most of simulated values agreed well with the measured values. The parametric study for the prototype rotary clap pump was conducted using the analysis model. The used parameters were the clearance between the rotor jaws and chambers, the number of jaws, the jaw width, and the jaw height, which are known as the important variables in the pump performance. Base on the parametric study, we found optimized condition that can increase overall efficiency up to 96.3%. The rotary clap pump generates relatively low pressure pulsation and can increase its displacement with low vibration and power loss compared to the reciprocating pump. This pump could be a better option for high-viscosity fluids at a high flow rate than any other positive-displacement pumps.

Manuscript received: July 27, 2016 / Revised: December 19, 2016 / Accepted: December 20, 2016

NOMENCLATURE

Δp_{FM}: Pressure head caused by the flowmeter, Pa
Q: Flow rate, m^3/sec
ρ: fluid density, kg/m^3
$f_{6\text{-}7,d}$, $f_{6\text{-}7,s}$: Friction factors in discharge and suction pipe
$l_{6\text{-}7,d}$, $l_{6\text{-}7,s}$: Length of discharge and suction pipe, m
$D_{6\text{-}7,d}$, $D_{6\text{-}7,s}$: Diameter of discharge and suction pipe, m
$Q_{6\text{-}7,d}$, $Q_{6\text{-}7,s}$: Flow rate in discharge and suction pipe, m^3/sec
$A_{6\text{-}7,d}$, $A_{6\text{-}7,s}$: Cross section area of discharge and suction pipe, m^2
K: Loss coefficient for pipe component
$h_{6\text{-}7,d}$, $h_{6\text{-}7,s}$: Height of discharge and suction pipe, m
δ_1, δ_2: Clearances between chamber and rotor jaws, m
N: Number of jaws
W_j: Width of jaw, m
h: Jaw height, m
η_v: Volumetric efficiency
η_t: Torque efficiency
η: Overall efficiency
$p_{7,d} - p_{6,d}$: Differential pressure in the discharge pipe, Pa
$p_{7,s} - p_{6,s}$: Differential pressure in the suction pipe, Pa
p_0: Gas charging pressure, Pa
p_m: Mean pressure of the pump system, Pa

1. Introduction

A novel rotary clap pump was developed to convert the positive-

displacement reciprocating pump actions into a rotary mechanism. There are two previous studies about the developed rotary clap pump: One described its structure and working principles through a kinematic analysis[1] and the other investigated pump performance such as pressure, driving torque, and efficiency characteristics by analytical methods using related theories.[2] In the former, important design parameters and their inter-relationships were analyzed. The determination of important variables such as crank radius, pin distance, gear teeth and rotor sizes considering mechanical constraints and inter-relation characteristics were studied, and it was found that the thickness angle of the jaw and inner radius of the rotor were the most significant constraints affecting the crank radius and pin distance of the mechanism. In the latter, the clearance between the rotor jaws and chambers, the number of jaws, the jaw width, and the jaw height were found to be important variables determining the pump performance.

In the two studies, we confirmed the operability and functionality of the rotary clap pump. However, those are analytical studies including some simplified assumptions. The experimental study is necessary to verify the developed analysis model, and to assure actual operational characteristics of the rotary clap pump.

In this study, an experimental verification was conducted for the prototype rotary clap pump. The pump performances derived from the analysis model and experiment were compared with each other. Parametric study and performance optimization to maximize the overall efficiency were also conducted using the verified analysis model. At the final step, the advantages of the rotary pump were discussed by comparing with conventional positive-displacement pumps.

2. Verification Test

2.1 Experimental setup

We manufactured a prototype pump with four rotor jaws to perform verification test. Its specifications are shown in Appendix A. The pump installed in test equipment as shown in Fig. 1, and the specifications of the piping system for the pump test are shown in Appendix B. A flowmeter, suction and discharge pressure sensors, torque meter, and speed sensor were used to measure the flow rate, suction and discharge pressures, input torque and speed of crank shaft, respectively. A throttle valve at the end of the discharge port is used to control the pressure at the pump. A geared motor and inverter were used to precisely control the input at low speed. The rated power and torque of the geared motor were 3.7 kW and 9.6 kgf·m, respectively, and the gear ratio was 1/5. The rated power of the inverter was 3.7 kW, and the efficiency was 98%. All sensor signals were stored in a laptop through a DAQ with eight analog and digital channels of a 32-bit resolution. The accuracy of the torque and speed sensors was 0.09%, and the signals were amplified by indicators. The measurement range of the flowmeter was 7.5~75 l/min. The oil temperature was maintained at 40°C by a temperature controller. Table 1 presents the specifications of the testing equipment.

2.2 Analysis model

We used four different kinds of piping components in the test equipment, i.e., nipple, ball valve, 90° elbow, and tee (Fig. 1). The numbers of each component used and their loss coefficients are in listed Table 2. The flowmeter on the discharge pipe also generated pressure head. Most manufacturers present pressure losses of a flowmeter

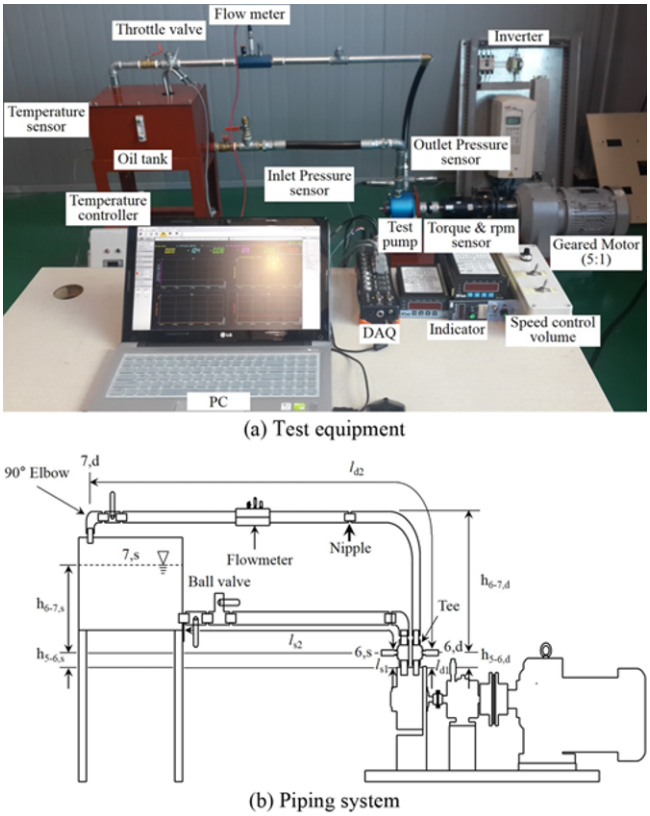

Fig. 1 The system used for pump testing

Table 1 Specifications of pump testing equipment

Items	Specifications
Geared motor	Model: Samyang Max II, 3 phase Power: 3.7 kW, Ratio: 1/5 RPM & Torque: 350 rpm & 94.18 N·m
Torque and rpm sensors	Model: SETech YDR-1K(torque) & MP-981(rpm) Type: Brush, Rated capacity: 9.8 N·m Accuracy: 0.09%
Pressure transducer	Model: sensys PSHB C010K Range: -0.01~0.98 MPa, Accuracy: 0.15%F.S
Flowmeter	Model: Hydrotechnik Hysense QT 110 Type: Volumetric, turbine Measuring range: 7.5~75 l/min Error limit: ±2.5% Allowed working pressure: 42 MPa Viscosity range: 1~100 mm^2/s
Inverter	Model: ABB ACS 800 Power: 3.7 kW, Efficiency: 98%
Test oil	Model: Kixx RD HD 32 ISO viscosity grade: ISO 32 Kinematic viscosity: 31.3 mm^2/s @40°C
DAQ	Model: DEWE-43 Power supply: 6-36 VDC Analog: No. of channels: 8 Sampling rate: simultaneous 200 kS/sec. Counter: No. of channels: 8 Resolution: 32 bit

Table 2 Loss coefficients for pipe connections[5,6]

Components	Suction line		Discharge line	
	No.	Coefficients	No.	Coefficients
Nipple	6 EA	0.85	6 EA	0.90
Ball valve	2 EA	0.07	1 EA	0.08
90° elbow	1 EA	0.69	1 EA	0.75
Tee	1 EA	0.46	1 EA	0.50

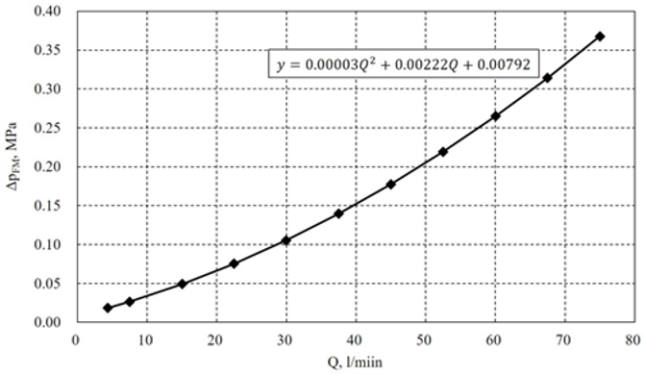

Fig. 2 Second-order polynomial model representing the differential pressure vs. flow rate of a flowmeter[4]

according to the flow rates. Fig. 2 shows a second-order polynomial regression model between flow rates and differential pressure provided by the manufacturer.[4] Accordingly, the pressure loss caused by the flowmeter can be expressed as follows.

$$\Delta p_{FM} = 0.00003Q^2 + 0.00222Q + 0.00792 \quad (1)$$

The total pressure losses in the discharge pipe from *6,d* to *7,d* can be expressed as Eq. (2) by adding the flowmeter effect to the analytical equation of previous study.[2]

$$p_{7,d} - p_{6,d} = \frac{1}{2}\rho\frac{f_{6-7,d}l_{6-7,d}}{D_{6-7,d}}\frac{Q_{6-7,d}^2}{A_{6-7,d}^2} + \rho l_{6-7,d}\frac{\dot{Q}_{6-7,d}}{A_{6-7,d}} + \frac{1}{2}\Sigma K\rho\frac{Q_{6-7,s}^2}{A_{6-7,s}^2} + (0.00003Q^2 + 0.00222Q + 0.00792)\times 10^{-6} \quad (2)$$

In the same way, the total pressure losses in the suction pipe from *6,s* to *7,s* can be expressed as Eq. (3).

$$p_{7,s} - p_{6,s} = \frac{1}{2}\rho\frac{f_{6-7,s}l_{6-7,s}}{D_{6-7,s}}\frac{Q_{6-7,s}^2}{A_{6-7,s}^2} + \rho l_{6-7,s}\frac{\dot{Q}_{6-7,s}}{A_{6-7,s}} + \frac{1}{2}\Sigma K\rho\frac{Q_{6-7,s}^2}{A_{6-7,s}^2} + \rho g h_s \quad (3)$$

The pressure in the pump and piping system can be simulated using Eqs. (2) and (3). Other analytical pump performance characteristics can be derived by directly using the equations of previous study.[2] The calculation with regard to the analysis model was conducted using Microsoft Excel.

2.3 Comparison of results derived from analysis model with experimental results

2.3.1 Flow rate, pressures, driving torque, and efficiencies

The clearances between the rotor jaws and pump chamber, δ_1 and δ_2, should be known to verify the pump performance of the rotary clap pump.[2] However, it is difficult to accurately measure those values. Therefore, we calculated them from the test results. Fig. 3 shows the measured flow rate as a function of the crank speed when the throttle valve was fully open. The analytical volumetric efficiency is also appeared in the numerical value, and it reached its maximum value when the crank speed was 125 rpm. Therefore, we calculated the clearances δ_1 and δ_2 based on that speed. We assumed δ_1 and δ_2 to have the same value. As a result, the volumetric efficiencies of the measured and simulated data had the same values when the clearances δ_1 and δ_2 were 0.2572 mm. Fig. 4 compares the test and simulated data for the volumetric efficiency as a function of the crank speed at that clearance values. Although we found some differences between the measured and simulated data when the crank speed were the lowest and the highest, in general the data showed good agreement. Therefore, we used 0.2572 mm of clearance values in the analysis model.

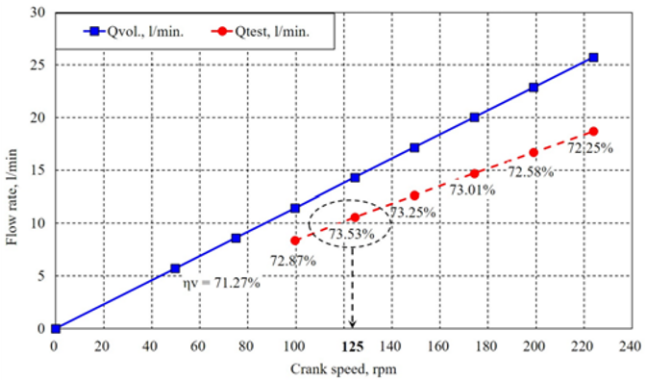

Fig. 3 Measured flow rate as a function of the crank speed with the throttle valve fully opened

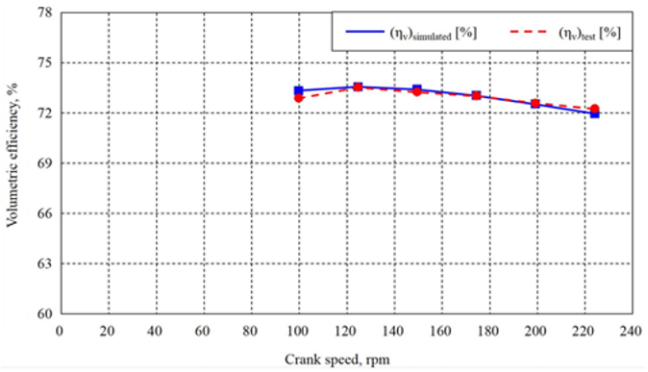

Fig. 4 Comparison between the measured and simulated volumetric efficiency as a function of the crank speed when the clearances δ_1 and δ_2 were 0.2572 mm

We verified the simulated data for the flow rate, differential pressure, and driving torque by comparison with experimental data under the same conditions. We measured the flow rate using a flowmeter installed between points *6,d* and *7,d*, as shown in Fig. 1. The suction and discharge pressure sensors were installed at points *6,s* and *6,d*, respectively. Therefore, we compared the measured and simulated pressures at those points. Fig. 5 shows the measured and simulated flow rates when the

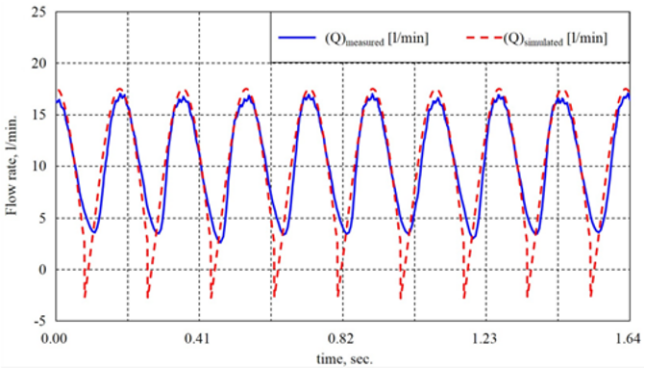

Fig. 5 Comparison between the simulated and measured flow rates in the time domain

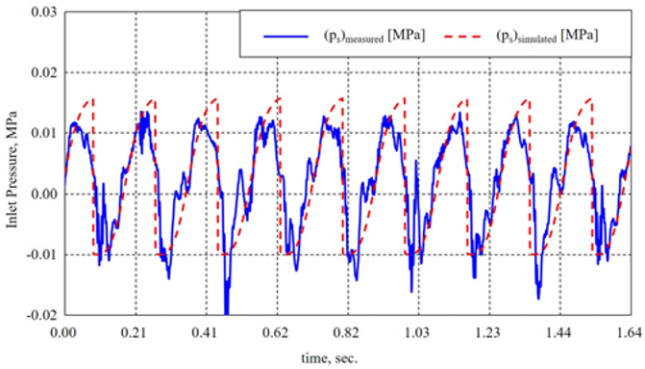

Fig. 6 Comparison between the simulated and measured suction pressures in the time domain

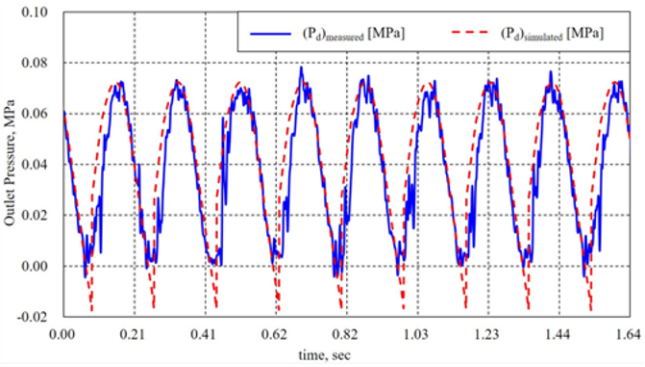

Fig. 7 Comparison between the simulated and measured discharge pressures in the time domain

speed of the driving shaft was 125 rpm. The measured and simulated values agreed well in terms of their magnitudes and periods. Figs. 6~8 compare the measured and simulated pressure and driving torque. These values also correlated well in terms of their magnitudes and periods.

Fig. 9 compares the measured and simulated efficiency characteristics of the prototype pump as a function of the crank speed when the throttle valve was fully open.

Although the simulated volumetric efficiency agreed well with the measured data, it was much lower than that of conventional pumps,

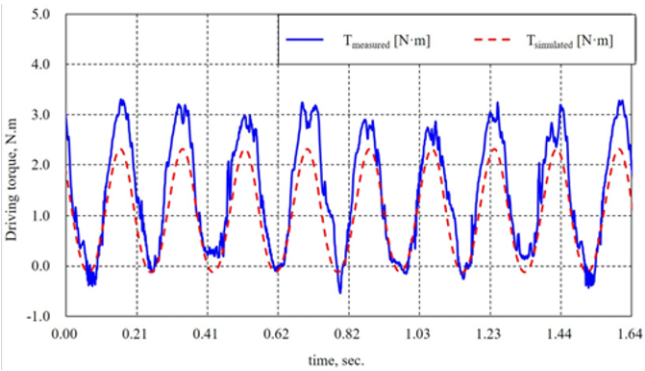

Fig. 8 Comparison between the simulated and measured driving torques in the time domain

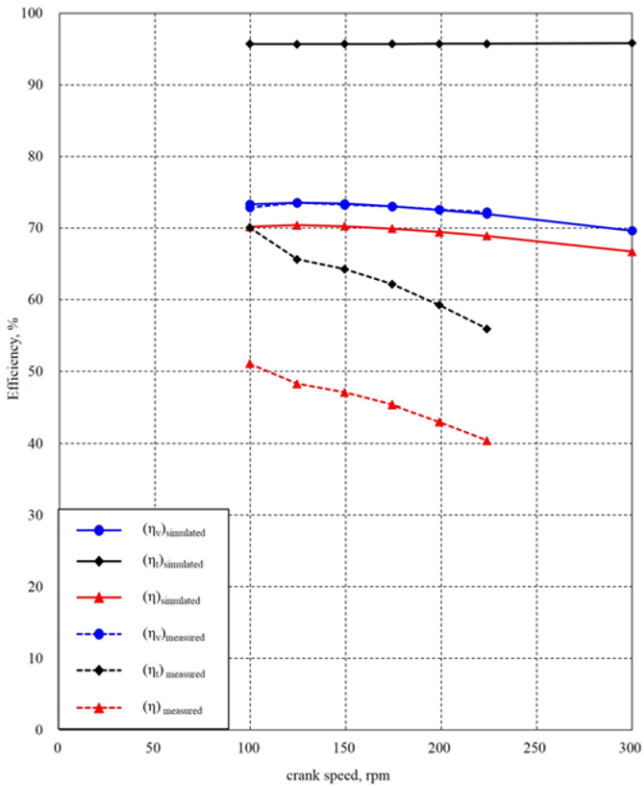

Fig. 9 Comparison between the measured and simulated pump efficiency as a function of the crank speed

possibly because the clearances between the pump chambers and rotor jaws were large. Fig. 10 shows the clearances between the pump chambers and rotor jaws, between 0.25 and 0.28 mm, as measured with a feeler gauge. That result agreed well with the simulated values.

On the other hand, the simulated torque efficiency did not agree with the measured data, and the difference increased with the crank speed. Mechanical friction in the pump is not considered in this study because the friction is relatively small in many practical cases.[3] Furthermore, abnormal mechanical friction caused by component misalignment, 0~0.2 mm, occurred periodically in the prototype pump as shown in Figs. 11 and 12. The misalignment of the components could have been aggravated as the differential pressure and crank speed

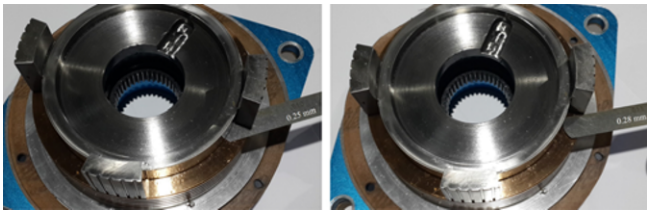

Fig. 10 Measurement of the clearances with a feeler gauge

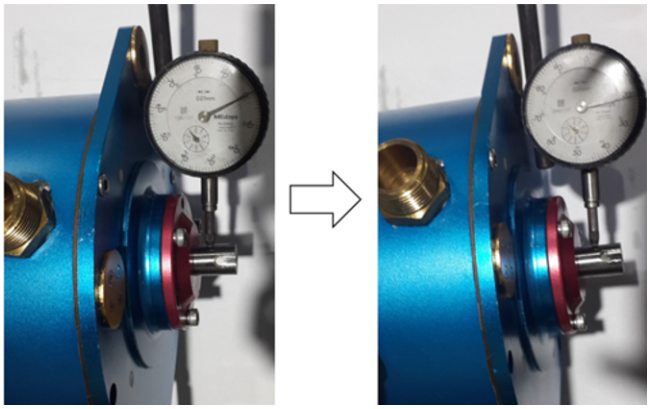

Fig. 11 Measurement of the crank misalignment with a dial gauge

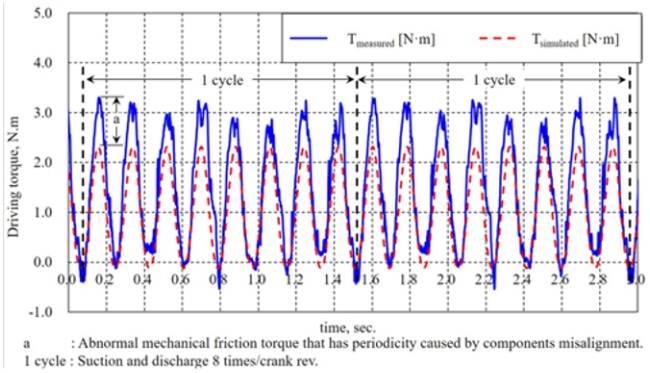

Fig. 12 Fluctuation of friction torque caused by the crank misalignment

increased. Therefore, we estimated that this misalignment of the components is the cause of the differences.

2.3.2 Pressure pulsation and cavitation

Pressure pulsation and cavitation are important factors, especially in positive-displacement pumps, because they have bad effects on the system. Cavitation can reduce delivery because vapor occupies a much larger volume than the liquid from which it is derived. In this case, the accompanying loss in delivery must not be confused with slip.[3] In positive-displacement pumps, cavitation can generally be decreased with pressure pulsation damping. The representative method for decreasing pressure pulsation is the use of multi-pumps or a pulsation dampener.

In the case of rotary clap pumps, pressure pulsation and cavitation are likely to occur because of their operational characteristics which cause large and frequent pressure changes. The effects of the multi-pumps and pulsation dampener to reduce a pressure pulsation are presented below.

Table 3 Effect of the number of pistons or rotor pairs on flow variation

Reciprocating pumps[7,8]			
No. of pistons	Above mean (%)	Below mean (%)	Total (%)
1	-	-	-
2	60	100	160
3	6.1	16.9	23
4	24	22	46
5	2	5	7
Rotary clap pumps			
No. of rotor pairs	Above mean (%)	Below mean (%)	Total (%)
1	62.3	99	161.3
2	9.6	18.4	28
3	4.4	8.3	12.7
4	2.9	4.8	7.7
5	1.6	2.9	4.5

Above mean: $(Q_{\max} - Q_{mean}) / Q_{mean} \times 100$
Below mean: $(Q_{\text{mean}} - Q_{min}) / Q_{mean} \times 100$
Total = Above mean + Below mean

2.3.2.1 Multi-pumps

In reciprocating pumps, pulsation can be reduced by adding multi-cylinders and timing the pumping strokes for small overlaps. The same method could reduce pressure pulsation in the rotary clap pump. Table 3 compares the effects of using different numbers of pistons on flow variations between the two types of pumps. It demonstrates that the pulsation of rotary clap pumps is smaller than that of reciprocating pumps with the same number of pistons (rotor pairs).

2.3.2.2 A pulsation dampener

Pulsation dampeners are frequently used to reduce piping pressure pulsations. However, there is no standard method for evaluating or ranking their effectiveness.[9,10] Therefore, the initial volume of a pulsation dampener is generally determined based on the experience of the manufacturer. The gas charging pressures are commonly determined as follows:[9]

$$0.5 p_m \le p_0 \le 0.8 p_m \quad (4)$$

To confirm the effect of the pulsation dampener on the rotary clap pump, we added them to the discharge and suction lines to the test equipment, as shown in Fig. 13. We also installed an air compressor to supply pressure in the pulsation dampeners.

Figs. 14 and 15 show the effects of the pulsation dampener on variations in the flow and discharge pressure. We used the pulsation dampener only during the second half of the test period. During the first half, the maximum, minimum, and mean flow rates were 35.18, 7.66, and 22 l/min, respectively. The total variation was 125%. In contrast, during the second half (with the dampener in use), the maximum, minimum, and mean flow rates were 21.26, 17.49, and 19.80 l/min, respectively. Thus, the total variation was 19%. In the same manner, the total variation in the discharge pressure was 220% and 61%, respectively. After a pulsation dampener was added, the flow fluctuation and discharge pressure pulsation were decreased to 15% and 28%, respectively, of the previous values. However, the mean flow rate and

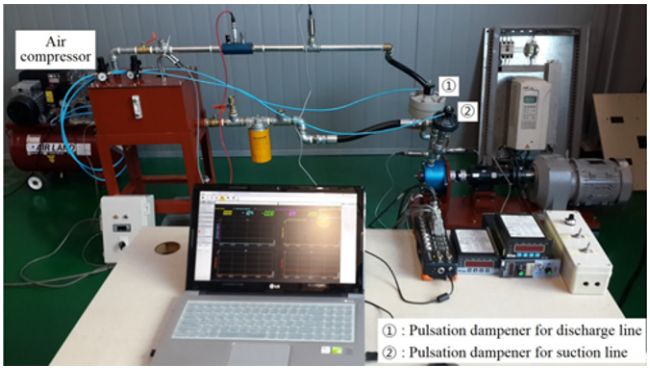

Fig. 13 Pulsation dampeners installed in the pump testing system

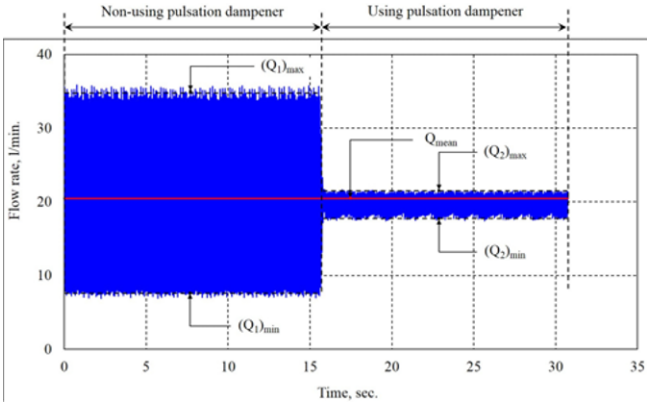

Fig. 14 Effect of the pulsation dampener on flow variations

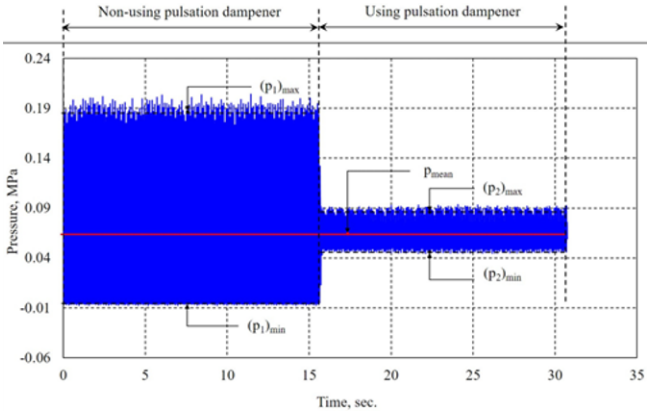

Fig. 15 Effect of the pulsation dampener on discharge pressure variations

discharge pressure decreased 10% more than before pulsation dampeners were used, indicating that cavitation in the suction line increased when using the pulsation dampeners, perhaps because the pulsation dampener was not optimized for the rotary clap pump conditions.

Fig. 16 compares the measured and simulated pressure-flow rate curves when the crank speed was 500 rpm. The dotted curve represents the simulated data considering the cavitation. We calculated the pressures based on the measured flow rate. It can be known that the simulated

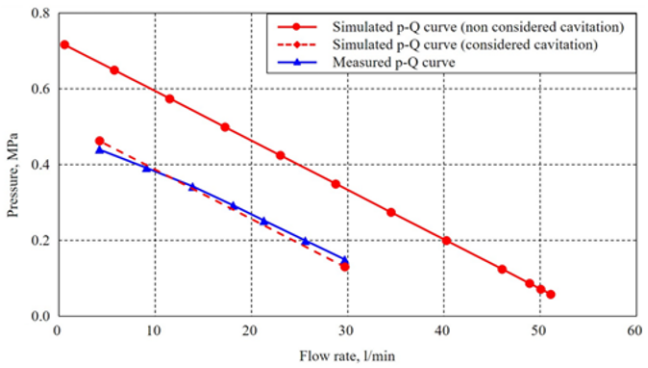

Fig. 16 Comparison between measured and simulated p-Q curves when the crank speed was 500 rpm

pressure was similar to the measured value.

Most of the simulated values agreed well with the measured data. Although there were some differences between the two results, we validated their causes, and as a result, our analysis model can be used to predict the clap pump performance. In addition, it could be predicted that the pressure pulsation and cavitation are smaller in the rotary clap pumps with double rotors and optimized pulsation dampeners than in the reciprocating pumps with triple pistons and pulsation dampeners.

3. Optimization of the Prototype Rotary Clap Pump Using Analysis Model

3.1 Parametric study

The number of jaws N, jaw width W_j, and jaw height h are the main parameters that affect pump performance of the rotary clap pump.[1,2] The parameters in appendix A that we used to design the prototype pump were not optimized. Therefore, we analyzed the effects of those parameters on pumping performance and optimized the prototype pump in the view of efficiency.

As discussed earlier, the clearances δ_1 and δ_2 between the jaws and chambers were calculated to be 0.2572 mm in the prototype pump. Those clearances are much larger than those of conventional pumps. The clearances influenced on the flow slip and the forces caused by the fluid viscosity.[2]

We compared the efficiencies as the clearances increased under the conditions given in appendix A. As shown in Fig. 17, the results showed that the volumetric efficiency decreased with the clearances, whereas the torque efficiency increased. The overall efficiency reached its maximum value when the clearances δ_1 and δ_2 were 0.06 mm.

We analyzed the efficiencies according to the jaw height h and number of jaws N under the clearances of 0.06 mm. The maximum volumetric, torque, and overall efficiencies were 98.98%, 96.07%, and 95.07% for jaw heights of 16, 14, and 14 mm, respectively. The torque and overall efficiencies increased with the number of jaws, but the volumetric efficiency decreased.

3.2 Optimization of the prototype pump

We here present performance predictions for several cases based on the analysis results.

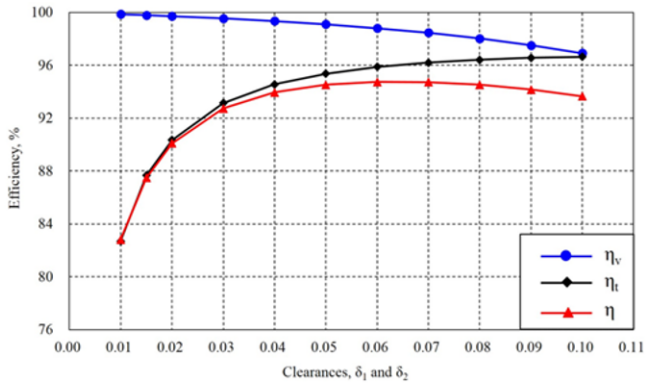

Fig. 17 Efficiency vs. clearance when n = 100 rpm, h = 10 mm, and N = 4

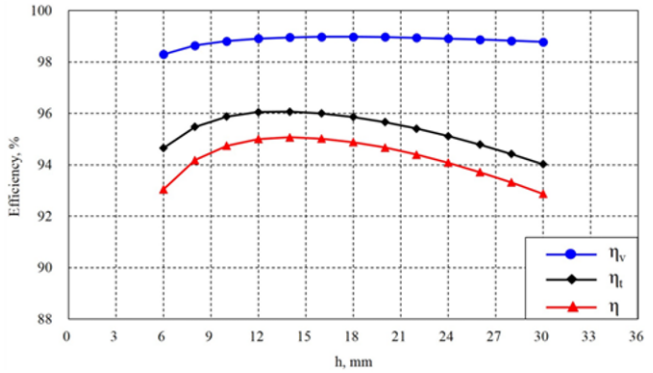

Fig. 18 Efficiency vs. jaw height when n = 100 rpm, $\delta_1 = \delta_2 = 0.06$ mm, and N = 4

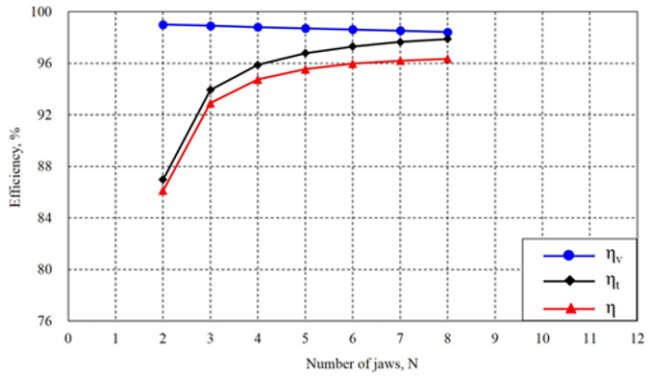

Fig. 19 Efficiency vs. number of jaws when n = 100 rpm, $\delta_1 = \delta_2 =$ 0.06 mm, and h = 10 mm

The first prediction was made under the following initial conditions.

1) We neglected the misalignment caused by manufacturing tolerances and did not consider mechanical friction.

2) The clearances between the jaws and chambers δ_1 and δ_2 were 0.2572 mm.

3) The other conditions are given in appendix A.

Thus, the initial state of the prototype pump did not invoke the problems discussed in 2.3.

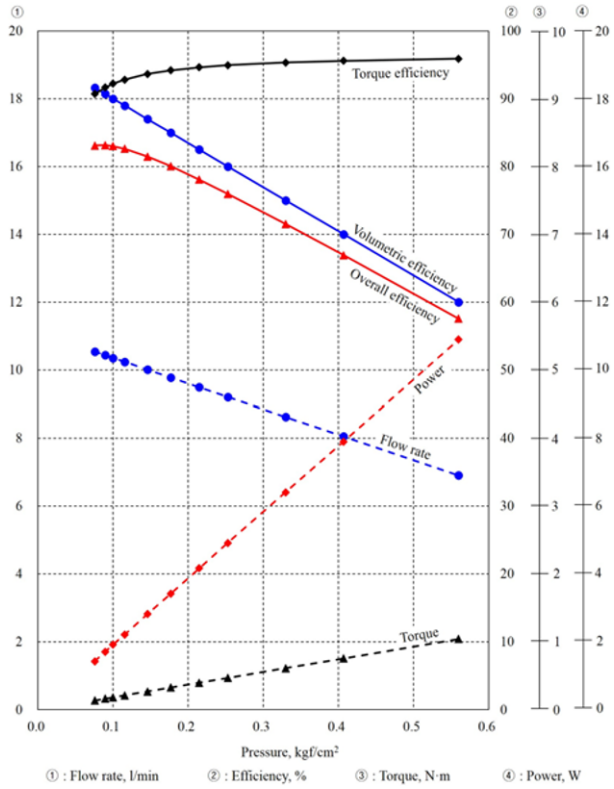

Fig. 20 Performance curves under the initial conditions (crank speed n = 100 rpm, clearance δ_1 and $\delta_2 = 0.2572$ mm)

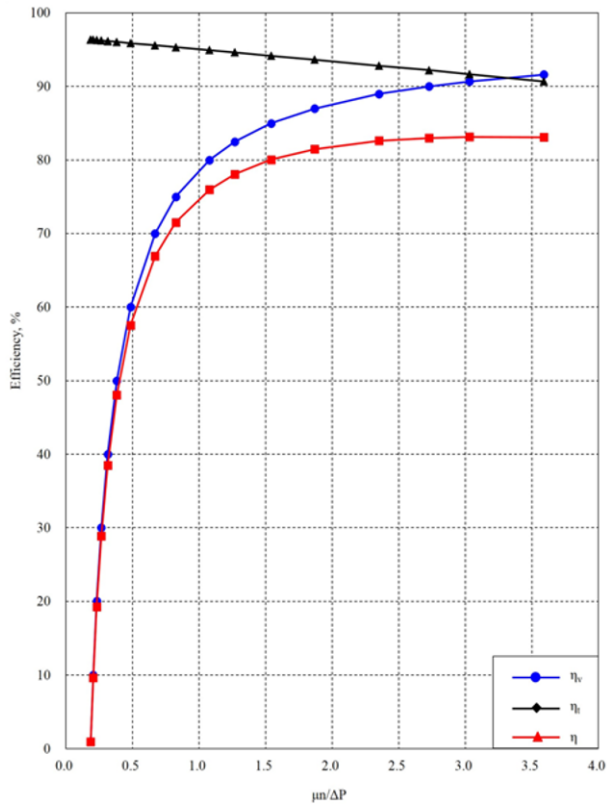

Fig. 21 Pump efficiency as a function of $\mu n/\Delta p$ under the initial conditions (crank speed n = 100 rpm, clearance δ_1 and $\delta_2 =$ 0.2572 mm)

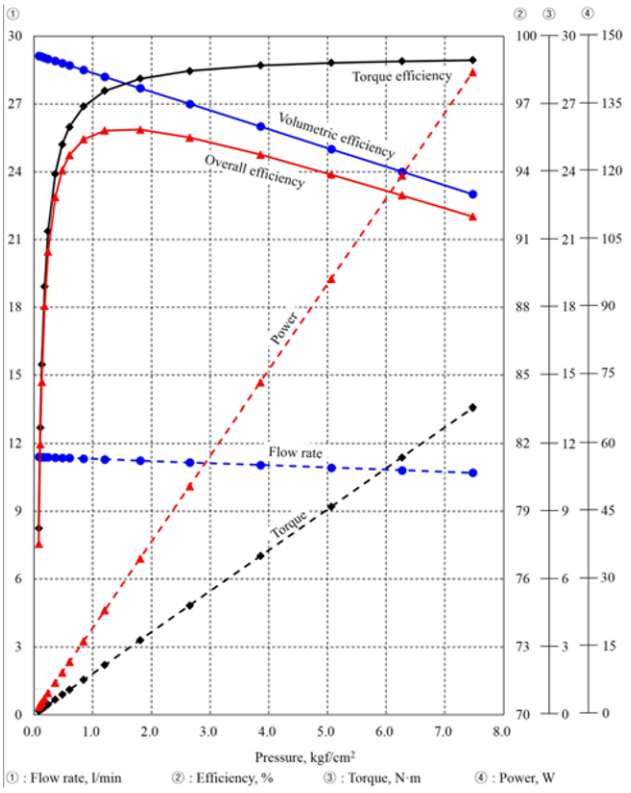

Fig. 22 Performance curves under the optimized clearance condition (crank speed n = 100 rpm, clearance δ_1 and δ_2 = 0.06 mm)

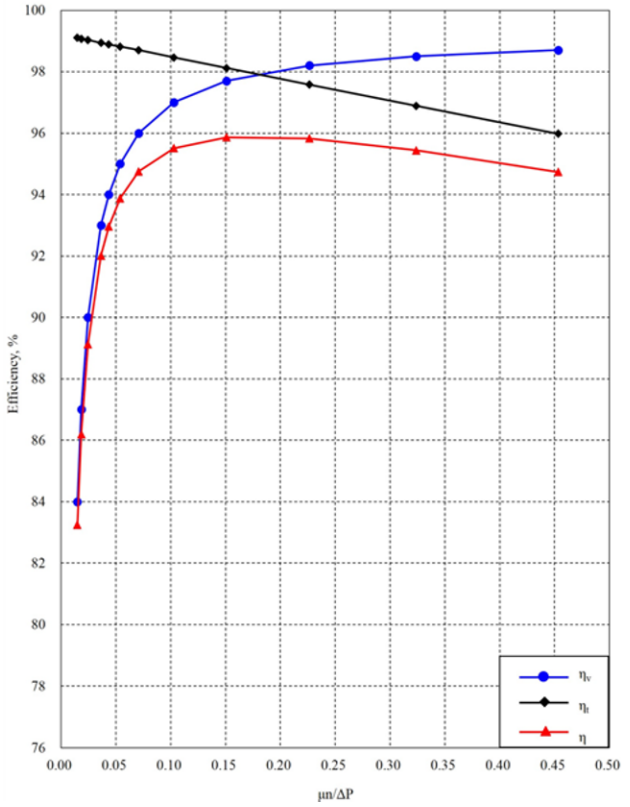

Fig. 23 Pump efficiency as a function of $\mu n/\Delta p$ under the optimized clearance condition (crank speed n = 100 rpm, clearance δ_1 and δ_2 = 0.06 mm)

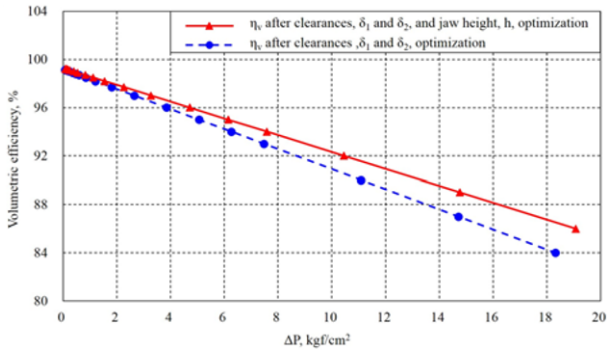

Fig. 24 Volumetric efficiency before and after jaw height optimization (crank speed n = 100 rpm)

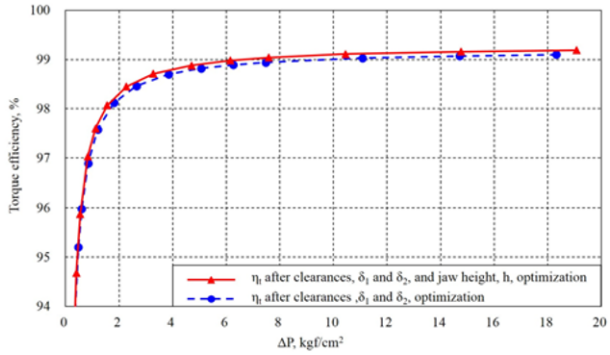

Fig. 25 Torque efficiency before and after jaw height optimization (crank speed n = 100 rpm)

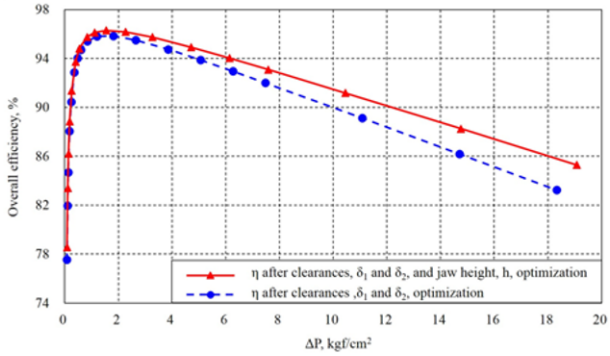

Fig. 26 Pump efficiency before and after jaw height optimization (crank speed n = 100 rpm)

Figs. 20 and 21 show the predicted performance curves and efficiency characteristics as a function of Δp and $\mu n/\Delta p_c$ under the initial conditions and crank speed n = 100 rpm. The overall efficiency was predicted to decrease from 83.11% to 57.54% as the differential pressure Δp increased from 0.08 kgf/cm^2 to 0.56 kgf/cm^2. The volumetric efficiency and overall efficiency were low because the clearances δ_1 and δ_2 were larger than those of conventional pumps. Therefore, our second performance curves assume clearances δ_1 and δ_2 with an optimized value of 0.06 mm. That change increased the maximum overall efficiency greatly from 83.14% to 95.86%. Figs. 22 and 23 show

the performance curves and efficiency characteristics as a function of Δp and $\mu n/\Delta p$ under optimized clearance values.

We next compare and analyze the performances before and after optimizing the jaw height h. As discussed in 3.1, the overall efficiency reached its maximum value when the jaw height h = 14 mm. Therefore, we predicted the efficiency again after increasing the jaw height h from 10 mm to 14 mm. Figs. 24~26 compare the efficiencies before and after jaw height optimization. All efficiencies after optimization are higher than those before. Figs. 27 and 28 show the predicted performance curves and efficiency characteristics as a function of Δp and $\mu n/\Delta p$ under the final conditions (optimized clearance and jaw height conditions) and crank speed n = 100 rpm. The predicted maximum overall efficiency was 96.3%.

4. Comparison between the Conventional Positive-Displacement Pumps and the Rotary Clap Pump

The main reasons for using positive displacement pumps are to move highly viscous fluid, maintain constant flow, obtain high vapor pressure conditions, and for self-priming. However, it is difficult to select from several positive-displacement pumps because they use many types of pumping principles. Some types of pumps can be suitable for a particular application, but other pumps might have limitations that prevent their use under a given condition. The most representative factors for selecting positive-displacement pumps are flow, pressure, viscosity, and temperature.[12]

Comparing conventional positive-displacement pumps and rotary clap pumps requires an understanding of the most representative feature of each pump. Fig. 29 compares cross-sections (chamber volumes) in the conveying chamber between the rotors and the housing for several types of pump. External and internal gears and vane pumps have a relatively small cross-section. Conversely, lobe and reciprocating pumps have a relatively large cross-section, therefore, they can easily be a compact size and reduce its rotational speed.

The parameters, h and W_j, of the rotary clap pump related to size of cross-section can adjust freely because they are not inter-related with other parameters of the mechanism.[1] Therefore, the rotary clap pump can be designed with having a larger cross-section than lobe and reciprocating pumps.

Shear stress of the pump is proportional to shear rate with a given viscosity.[2] The shear rate is dv/dy. This term is an important factor in pumps when moving highly viscous or shear-sensitive fluid. It is not good for a pump to increase its shear rate. Highly viscous fluid can generate a large amount of viscous torque when it passes through the chamber of a pump. Furthermore, a shear-sensitive fluid's properties can be altered. Therefore, shear rate should be kept as low as possible. The two main ways to minimize shear rate are to decrease pump speed and increase the cross-section of the conveying chamber between the rotors and the housing. In this respect, the rotary clap pump is structurally good. It can be used with high-viscosity fluid, a high flow rate, and low and middle pressure, as shown in modified Table 4, which was originally presented in a previous study.[3] Table 5 shows comparisons among the conventional positive-displacement and rotary clap pumps using common and representative features from the literature.[3,7,11-14]

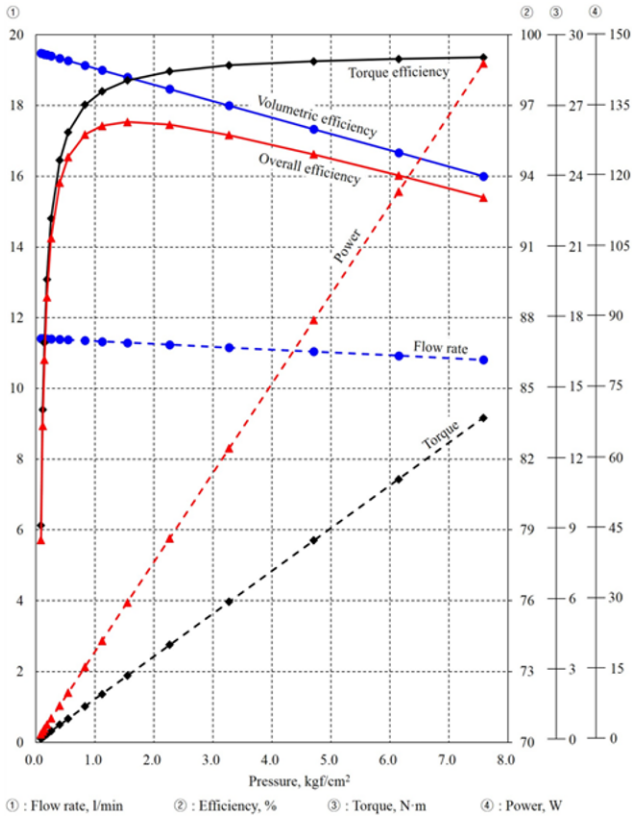

Fig. 27 Performance curves under the optimized clearance and jaw height conditions (crank speed n = 100 rpm)

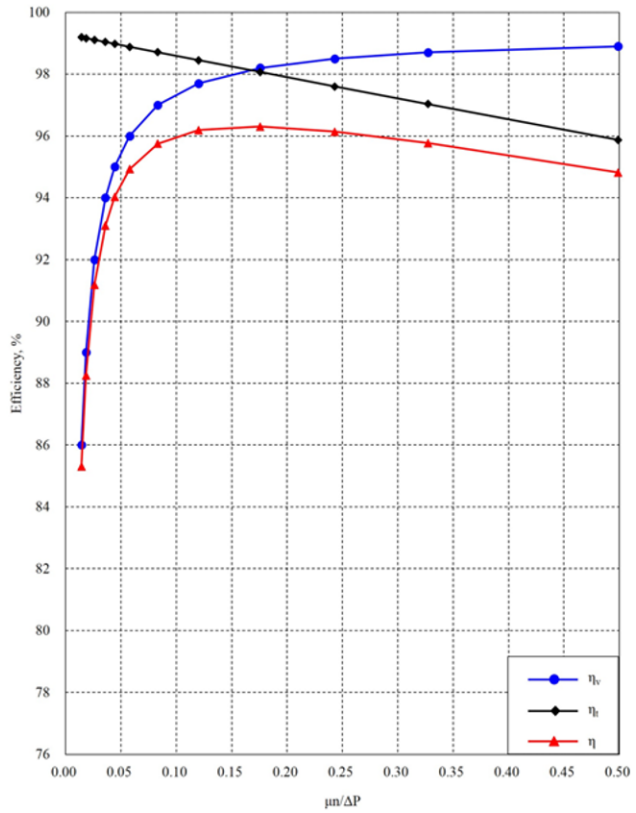

Fig. 28 Pump efficiency as a function of $\mu n/\Delta p$ under the optimized clearance and jaw height conditions (crank speed n = 100 rpm)

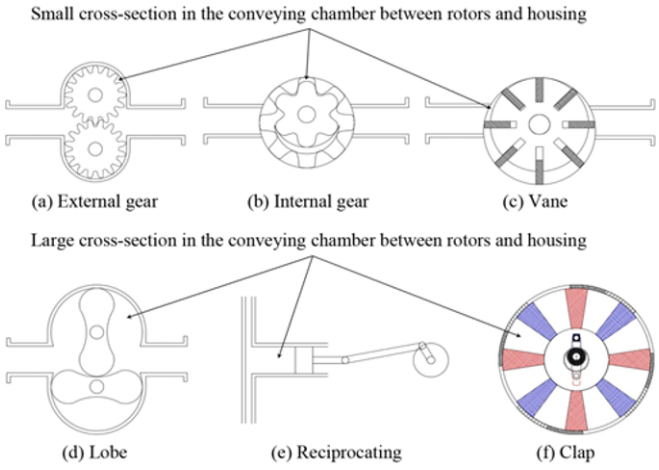

Fig. 29 Space between different types of rotors and their housings

Table 4 Serviceability of positive-displacement pumps

Pressure	Delivery		
	Low	Middle	High
Low	Gear Vane Multi-piston	Vane Lobe Gear	Lobe Rotary clap
Middle	Gear Vane Multi-piston	Vane Multi-piston Gear	Low speed single piston Rotary clap
High	Multi-piston	Multi-piston	Low speed single piston

Table 5 Characteristics of conventional positive-displacement pumps and the rotary clap pump

	MC	MP	MV	P	Other features
V	N	N	B	G	· Good for thick liquids · Can run dry for short periods
EG	N	N	N	G	· Simple · Bi-directional · High speed
IG	N	N	N	G	· Adjustable end clearance · Bi-directional
L	G	B	G	N	· Low shear · No metal-to-metal contact · Pass medium solids · Bi-directional
R	N	VG	B	VB	· High pressure capability · Excellent metering capability
RC	G	N	G	B	· Large cross-section · Low shear · Internal clearances can be adjusted freely · Bi-directional

· MC: Max. Capacity, MP: Max. Pressure, MV: Max. Viscosity, P: Pulsation, V: Vane, EG: External Gear, IG: Internal Gear, L: Lobe, R: Reciprocating, RC: Rotary Clap, VG: Very good, G: Good, N: Normal, B: Bad, VB: Very bad

5. Conclusions

The analysis model for the rotary clap pump was verified through a prototype experiment. The important pumping performances such as flow rate, differential pressure, driving torque, and efficiencies were selected as verification parameters. The parameters were derived from both analysis model and experiment, and the comparison of the two results was performed for the purpose of this study. Most of the simulated values agreed well with the measured data. Although there were some differences between the two results, we validated their causes, and as a result, our analysis model can be used to predict the clap pump performance.

Using the verified analysis model, we optimized the prototype pump by parametric study of the important design variables such as number of jaws, jaw width, and jaw height. The overall efficiency of prototype pump increased up to 96.3% through this optimization.

The effect of pulsation dampener to reduce a pressure pulsation was also evaluated experimentally. In the results, the total variation in the discharge pressure and flow rate decreased with a pulsation dampener. However, the mean flow rate and discharge pressure decreased 10% and 17.7% compared to without a pulsation dampener, indicating that cavitation in the suction line increased with the pulsation dampener.

The rotary clap pump showed typical characteristics of the positive-displacement rotary pump. This pump generated relatively low pressure pulsation and can increase its displacement with low vibration and power loss compared to the reciprocating pump. This pump could be a better option for high-viscosity fluids at a high flow rate than any other positive-displacement pumps.

ACKNOWLEDGEMENT

This work was supported by Korea Institute of Planning and Evaluation for Technology in Food, Agriculture, Forestry and Fisheries (IPET) through Agriculture, Food and Rural Affairs Research Center Support Program, funded by Ministry of Agriculture, Food and Rural Affairs (MAFRA) (716001-7).

REFERENCES

1. Shim, S. B., Park, Y. J., Kim, J. M., and Kim, K. U., “Development of a Rotary Clap Mechanism for Positive-Displacement Rotary Pumps: Kinematic Analysis and Working Principle,” Journal of Mechanical Science and Technology, Vol. 29, No. 2, pp. 759-767, 2015.
2. Shim, S.-B., Park, Y.-J., Nam, J.-S., Kim, S.-C., Kim, J.-M., and Kim, K.-U., “Development of a Rotary Clap Mechanism for Positive-Displacement Rotary Pumps: Pumping Performance Analysis,” Int. J. Precis. Eng. Manuf., Vol. 18, No. 4, pp. 575-585, 2017.
3. Wilson, W. E., “Positive-Displacement Pumps and Fluid Motors,” Pitman Publishing Corporation, 1950.
4. Hydrotechnik GmbH, “HySense QT 100 / QT 110,” http://www.hydrotechnik.co.uk/sites/hydrotechnik.co.uk/files/catpdf/QT100_(RE4)_Turbines.pdf (Accessed 8 MAR 2017)
5. Hydraulic Institute, “Hydraulic Institute Engineering Data Book,”

Hydraulic Institute, 2nd Ed., 2015.

6. Menon, E. S. and Menon, P., "Working Guide to Pumps and Pumping Stations," Oxford, Linacre House, Jordan Hill, 2010.
7. Karassik, I. J., Krutzsch, W. C., Fraser, W. H., and Messina, J. P., "Pump Handbook," McGraw-Hill Education, 4th Ed., 2007.
8. Thompson, D. J., "Using a Pulsation Dampener with a Reciprocating Pump," Pumps&Systems, pp. 26-29, 2006. http://yuypump.com/tools/download.ashx?site=main&id=2483 (Accessed 8 MAR 2017)
9. Lee, I. Y,. "Hydraulic Engineering," Munundang, 2012. (in Korean)
10. Singh, P. J. and Chaplis, W. K., "Experimental Evaluation of Bladder Type Pulsation Dampeners for Reciprocation Pumps," Proc. of the 7th International Pump Users Symposium, pp. 39-48, 1990.
11. Petersen, J. E., "Best Practices in Selecting and Applying Positive Displacement Pumps," Proc. of the International Pump Users Symposium, pp. 109-118, 2001.
12. William, E. F., "Forsthoffer's Rotating Equipment Handbooks: Pumps," Elsevier Science, 2005.
13. Hourse, A., Jackson, J. K., Langreau, R. R., Martin, C., Miller, S. G., et al., "Types of Pumps," in: Pumping Station Design, Jones, G. M., Sanks, R. L., (Eds.), Elsevier, 3rd Ed., Chap. 11, 2008.
14. Volk, M., "Pump Characteristics and Applications," CRC Press, 2nd Ed., 2005.

APPENDIX

Appendix A Specification of the rotary clap pump used in the performance test

Parameters		Values
Performance	Flow rate	11.5 l/min@100 rpm
	Max. differential pressure	5 kgf/cm^2
	Kinematic viscosity of fluid	32 mm^2/sec
Kinematic	No. of rotor jaws	4
	Crank radius r_c	4 mm
	Distance between pins P_1 and P_2 L	64.6 mm
	Maximum relative angular displacement between rotors 1 and 2 $(\theta_{rel})_{max}$	26°
	Jaw width W_j	30 mm
	Jaw height h	10 mm
	Outer radius of rotor r_o	53.5 mm
	Gear module m	1
	No. of teeth on the gear of the shaft link Z_p	30
	No. of teeth on the fixed internal gear Z_r	40
	Reference pressure angle α	25°
	Moment of inertia of the rotors I_R	9.99×10^{-4} kg·m^2

Appendix B Specifications of piping system for the pump test

Common parameters					
ρ	855.00		kg/m^3		
f	64/Re		Re : Reynolds's number		
Suction line parameters			Discharge line parameters		
$l_{1\text{-}2,s}$	variation		$l_{1\text{-}2,d}$	variation	
$l_{2\text{-}3,s}$	0.0050	m	$l_{2\text{-}3,d}$	0.0050	m
$l_{3\text{-}4,s}$	0.0065	m	$l_{3\text{-}4,d}$	0.0065	m
$l_{4\text{-}5,s}$	0.0100	m	$l_{4\text{-}5,d}$	0.0100	m
$l_{5\text{-}6,s}$	0.0700	m	$l_{5\text{-}6,d}$	0.0600	m
$l_{6\text{-}7,s}$	1.2400	m	$l_{6\text{-}7,d}$	1.8700	m
$A_{1\text{-}2,s}$	0.00120	m^2	$A_{1\text{-}2,d}$	0.00120	m^2
$A_{2\text{-}3,s}$	0.00038	m^2	$A_{2\text{-}3,d}$	0.00025	m^2
$A_{3\text{-}4,s}$	0.01678	m^2	$A_{3\text{-}4,d}$	0.01510	m^2
$A_{4\text{-}5,s}$	0.00051	m^2	$A_{4\text{-}5,d}$	0.00029	m^2
$A_{5\text{-}6,s}$	0.00051	m^2	$A_{5\text{-}6,d}$	0.00029	m^2
$A_{6\text{-}7,s}$	0.00051	m^2	$A_{6\text{-}7,d}$	0.00029	m^2
$h_{5\text{-}6,s}$	-0.07	m	$h_{5\text{-}6,d}$	0.07	m
$h_{6\text{-}7,s}$	-0.35	m	$h_{6\text{-}7,d}$	0.6	m
$W_{1\text{-}2,s}$	0.0300	m	$W_{1\text{-}2,d}$	0.0300	m
$W_{2\text{-}3,s}$	0.0120	m	$W_{2\text{-}3,d}$	0.0080	m
$W_{3\text{-}4,s}$	0.0400	m	$W_{3\text{-}4,d}$	0.0360	m
$D_{h1\text{-}2,s}$	0.0598	m	$D_{h1\text{-}2,d}$	0.0598	m
$D_{h2\text{-}3,s}$	0.0174	m	$D_{h2\text{-}3,d}$	0.0128	m
$D_{h3\text{-}4,s}$	0.0730	m	$D_{h3\text{-}4,d}$	0.0663	m
$D_{4\text{-}5,s}$	0.0254	m	$D_{4\text{-}5,d}$	0.0191	m
$D_{5\text{-}6,s}$	0.0254	m	$D_{5\text{-}6,d}$	0.0191	m
$D_{6\text{-}7,s}$	0.0254	m	$D_{6\text{-}7,d}$	0.0191	m
$\sum K_{1\text{-}2,s}$	0.00		$\sum K_{1\text{-}2,d}$	0.00	
$K_{2,s}$	Variation		$K_{2,d}$	Variation	
$\sum K_{2\text{-}3,s}$	0.00	-	$\sum K_{2\text{-}3,d}$	0.00	-
$\sum K_{3\text{-}4,s}$	0.00	-	$\sum K_{3\text{-}4,d}$	0.00	-
$\sum K_{4\text{-}5,s}$	0.00	-	$\sum K_{4\text{-}5,d}$	0.00	-
$\sum K_{5\text{-}6,s}$	0.85	-	$\sum K_{5\text{-}6,d}$	0.90	-
$\sum K_{6\text{-}7,s}$	5.54	-	$\sum K_{6\text{-}7,d}$	5.83	-